Applied Computer Science, vol. 18, no. 3, pp. 31–41
doi: 10.35784/acs-2022-19

Submitted: 2022-07-22 | Revised: 2022-09-01 | Accepted: 2022-09-23

Keywords: cavitation, CFD, fluid flow, hydrodynamics, orifice, simulation

Konrad PIETRYKOWSKI [0000-0001-6497-7572]*,
Paweł KARPIŃSKI [0000-0001-5786-1248]*

SIMULATION STUDY OF HYDRODYNAMIC CAVITATION IN THE ORIFICE FLOW

Abstract

Hydrodynamic cavitation is a phenomenon that can be used in the water treatment process. For this purpose, venturis or orifices varying in geometry are used. Studying this phenomenon under experimental conditions is challenging due to its high dynamics and difficulties in measuring and observing the phase transition of the liquid. For this reason, the CFD method was used to study the phenomenon of hydrodynamic cavitation occurring in water flow through the orifice and then analyze flow parameters for different boundary conditions. The research was performed for four different orifice geometries and two defined fluid pressure values at the inlet, based on a computational 2D model of the research object created in Ansys Fluent software. As a result of the numerical simulation, the distribution of fluid velocity and pressure and volume fraction of the gas phase were obtained. A qualitative and quantitative analysis of the phenomenon of hydrodynamic cavitation under the considered flow conditions was conducted for the defined orifice geometries. The largest cavitation zone and thus the largest volume fraction of the gas phase was obtained for the orifice diameter of 2 mm with a sharp increase in diameter. However, the geometry with a linear change in diameter provided the largest volume fraction of the gas phase per power unit.

1. INTRODUCTION

The phenomenon of cavitation is a rapid phase transition of the fluid from the liquid to gaseous phase due to a decrease in pressure. According to the principle of energy conservation in hydrodynamics (Bernoulli's law), if the velocity of the fluid increases, then the static pressure decreases. Cavitation occurs if the static pressure of the fluid below the saturated vapor pressure is reduced and then increased above this limit. Then the evaporation and formation of gas bubbles will occur, followed by their implosion. Bubble behavior formed during cavitation was studied (Moholkar & Pandit, 1997) and it was observed that the behavior of gas bubbles changes drastically under turbulent flow conditions. Numerical studies (Gogate & Pandit, 2000) showed that bubble dynamics, and thus the pressure created when bubbles collapse, depends on parameters such as the inlet pressure through the orifice system, the initial size of the cavity and the diameter of the orifice which affects the frequency of turbulence in the reactor.

* Lublin University of Technology, Faculty of Mechanical Engineering, Department of Thermodynamics, Fluid Mechanics, and Aircraft Propulsion Systems, Lublin, Poland, wm.ktmp@pollub.pl

Cavitation is a phenomenon that can be used in various industrial applications involving physical or chemical transformations. This phenomenon can form hydrodynamic, acoustic, optical, and particle cavitation (Gogate, Tayal & Pandit, 2006). Cavitation can improve the biological oxidation of natural municipal and industrial wastewater (Gogate, Thanekar & Oke, 2020). Orifices or venturi with different geometries can be used to generate hydrodynamic cavitation. Orifices in the form of a venturi can vary in length and diameter.

Hydrodynamic cavitation finds particular application in industrial water treatment processes. Moreover, their number and distribution on the cavitation inducer disc can vary. This phenomenon makes it possible to remove various chemical pollutants, for example, ammoniacal nitrogen (Patil, Bhandari & Ranade, 2021). Scientific papers on hydrodynamic cavitation for wastewater treatment (Wang, Su & Zhang, 2021) and the oxidation of organic compounds contained in industrial wastewater (Gągol, Przyjazny & Boczkaj, 2018) were reviewed in detail. For the analysis of processes using the phenomenon of cavitation, models linking the dynamics of the bubbles formed to chemical reactions play an essential role (Tao et al., 2016). An example of such a model is the hydrodynamic cavitation model, including radical hydroxyl production (Capocelli et al., 2014).

The cavitation phenomenon in Venturi tubes was studied (Shi et al., 2019). The experimental results were compared with the simulation calculations of venturis with the convergence angles of 19 and 45 degrees, respectively. The results showed that changing the convergence angle significantly affects flow characteristics and cavitation generation. It was shown that a 45-degree convergence angle enhances cavitation compared to the smaller angle tested. The results developed a semi-empirical model to predict cavitation in venturis.

Cavitation flows are associated with phase transitions resulting in significant and rapid density changes in low-pressure regions (Singhal et al., 2002). In addition, this type of flow is sensitive to the formation and transport of vapor bubbles and turbulent velocity and pressure fluctuations. These aspects were included in the cavitation model developed by Singhal. The phase-change rate was considered in terms of rates derived from a reduced form of the Rayleigh-Plesset equation for bubble dynamics. In general, this equation is a differential equation that allows for the calculation of bubble radius as a function of fluid pressure change (Franc, 2006). A cavitation model based on the multi-phase flow equations was developed (Zwart, Gerber & Belamri, 2004) and validated by testing flow through a venturi.

The study of cavitation flow under experimental conditions can be complex due to the high dynamics of accompanying phenomena and the associated difficulties in measuring and observing fluid phase transitions so computational fluid mechanics (CFD) is used to study such issues. This method makes it possible to analyze flow parameters for various boundary conditions. Its great advantage is the low cost of conducting research and performing a series of calculations in a short time compared to empirical studies.

Cavitation is often studied for industrial applications such as injectors, propellers, and water pumps. The simulation study of the cavitation phenomenon in a model water pump (Ding et al., 2011) shows that the predicted pump performance and cavitation characteristics obtained from the CFD method matched well with the experimental results. For CFD calculations, there may be certain difficulties in multi-phase and cavitation models. In the case of a simulation study of cavitation in a positive displacement pump, the calculated evaporation/condensation rate and the fundamental dynamics of the phenomenon may be

inconsistent due to an inaccurate calculation of the expansion of non-condensable gas (Iannetti, Stickland & Dempster, 2016). The CFD method was also used to model the flow of submerged bodies subjected to natural and ventilated cavitation (Kunz et al., 1999). The CFD method can also study cavitation resulting from propeller flow (Subhas et al., 2012). Various computational solvers such as RANS, LES, and BEM can be used to study propeller cavitation modeling (Salvatore, Streckwall & Van Terwisga, 2009). Studies showed that mesh resolution in the cavitation flow region and numerical dispersion is essential for predicting the range and dynamics of cavitation.

A dimensionless parameter for evaluating cavitation is the cavitation number. This parameter can be determined for any flow although the cavitation phenomenon does not always have to occur. The value of the cavitation number corresponding to the first occurrence of cavitation at a given inlet pressure is referred to as the cavitation inception number (Brennen, 1994). Cavitation initiation is sensitive to nozzle geometry changes (Omelyanyuk, 2022). As noted, geometric parameters are not included in the cavitation number formula so cavitation initiation can occur differently with the same cavitation number. The analyses performed were based on CFD calculations compared with experimental results.

This work discusses a simulation study of hydrodynamic cavitation in fluid flow through four orifices with varied geometries for two defined fluid pressure values at the inlet. For this purpose, a computational 2D model was developed in Ansys Fluent software and its assumptions are presented in Section 2. As a result of numerical calculations, the distribution of fluid velocity and pressure and volume fraction of the gas phase were obtained and underwent quantitative and qualitative analysis. The results and analysis are presented in Section 3. Finally, Section 4 summarizes the research and considerations on the cavitation phenomenon.

2. METHOD AND RESEARCH OBJECT

The phenomenon of hydrodynamic cavitation resulting from water flow through four orifices with different geometries was analyzed numerically (Fig. 1). The first of the geometries, marked as A, was characterized by a single diameter. The orifice channel of a diameter of 1 mm and a length of 5 mm was straight and its origin was at a distance of 10 mm from the inlet surface. The overall length of the computational domain was 25 mm. The second geometry, designated B, had a larger diameter of 2 mm. The following orifice geometries had a gradually increasing diameter. In geometry C, the initial diameter of 1 mm and a length of 1.5 mm increased to 1.5 mm. In geometry D, the change in diameter was sharp and its value changed from 2 to 2.5 mm. The change occurred at a distance of 1 mm from the edge of the inlet. The overall lengths of the orifices and the computational domain were the same in all cases considered. A 2D model was analyzed due to its axisymmetric design. This approach significantly reduces the time of numerical calculations without affecting the results.

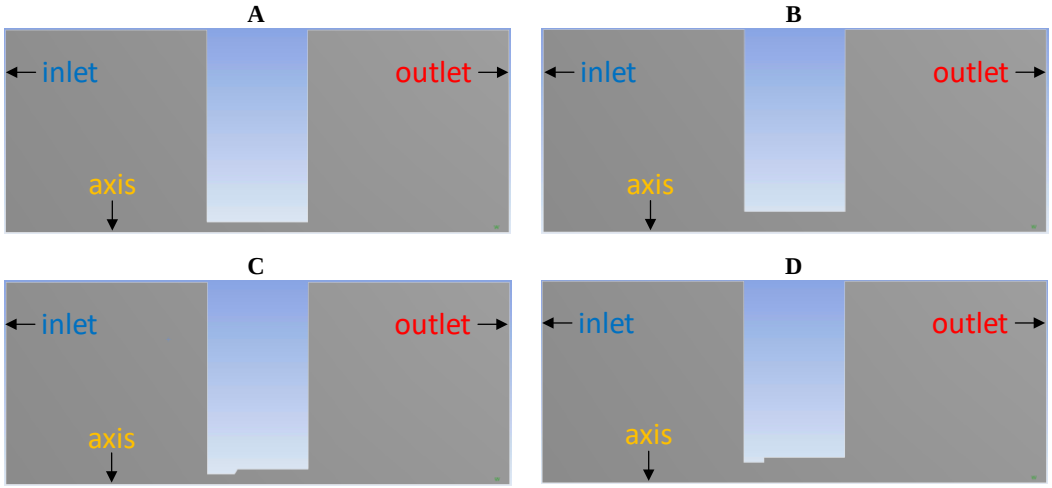

Fig. 1. Geometric models of the studied orifices

The 2D model was developed for the considered orifice geometries to analyze flow parameters in Ansys Fluent software. The computational meshes of 16 095, 17 000, 17 404, and 17 047 cells were generated, respectively. The cells were quadrilateral and triangular and ranged from 0.1 to 0.2 mm. Within a radius of 2.5 mm from the edge of the hole inlet, the cells were concentrated at 0.06 mm. In addition, a wall layer composed of ten 0.5 mm thick layers with a growth rate of 1.2 was created on the wall of the modeled orifice. Fig. 2 shows the generated meshes.

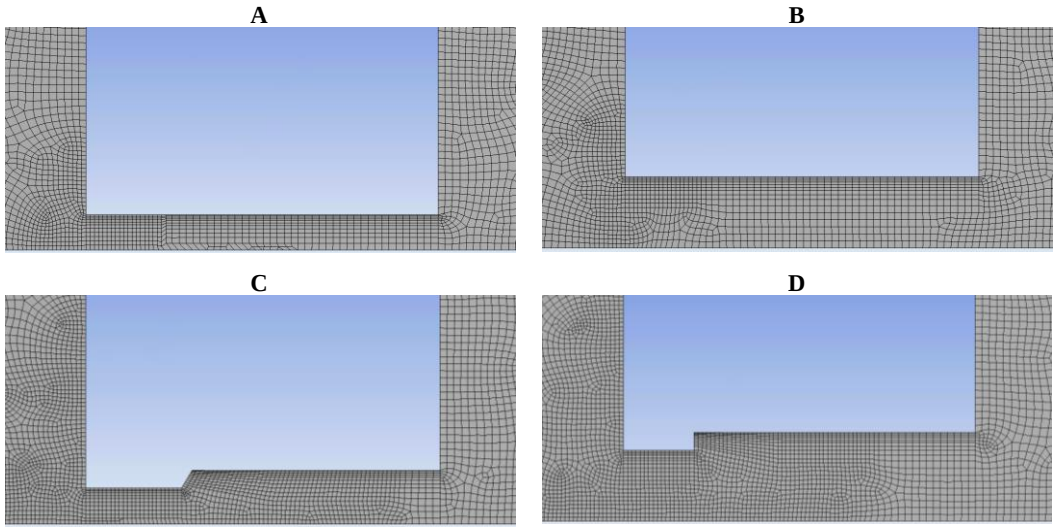

Fig. 2. Generated computational meshes for the tested orifice geometries

A mixture-type multi-phase model was used to simulate the cavitation process and two phases, i.e. liquid water and gaseous water were defined. The Schnerr-Sauer cavitation model was chosen, and a cavitation pressure of 3 540 Pa was set. This pressure value represents the pressure of saturated vapor at 300 K. In addition, the model assumed a constant

density of the liquid phase of 998.2 kg/m^3 and the gas phase of 0.8 kg/m^3. This is necessary due to the difficulty of achieving convergence of calculations when compressibility of the gas phase is assumed. The model includes the gas phase, the liquid phase, and the processes of evaporation and condensation of the liquid (Zheng et al., 2018). The model uses the Volume-of-Fluid method (VOF) which is used to predict the growth and collapse of resulting bubble clouds (Sauer & Schnerr, 2001; Schnerr & Sauer, 2001). The k-ω SST model was adopted as the turbulence model. This k-ω model represents the turbulent flow in the near-wall layer well and remains sensitive to the amount of turbulence in the free flow. Therefore, a shear stress transport (SST) model was used, which allows transition to the k-ε model in the free flow while modeling the boundary layer using k-ω. The turbulence model includes kinetic energy k and turbulence-specific dissipation rate ω (Menter, 1993; Menter, 1994). A correct modeling of the near-wall layer is desirable because the cavitation phenomenon occurs exactly in this flow zone. The boundary conditions were inlet pressures of 700 kPa and 1 000 kPa and outlet pressure of 100 kPa. The calculations were performed until convergence equivalent to a maximum residuals level of $1 \cdot 10^{-5}$.

3. RESULTS AND DISCUSSION

Numerical calculations made it possible to obtain velocity, pressure, and volume fraction distributions of the gas phase for four considered orifice geometries for the two defined inlet pressures: 700 kPa and 1 000 kPa. The adopted pressure values result from the conclusions drawn from preliminary tests of the developed water treatment system. On the one hand, the maximum pressure value is limited due to the high energy consumption of the system, but on the other hand, the minimum value stems from the satisfactory treatment results obtained at this pressure value.

The first parameter analyzed was velocity distribution. The results in the form of streamlines for the considered orifice geometries and inlet pressures are shown in Fig. 3 and Fig. 4. The colors of the streamlines show the flow velocity in the model. For the lower pressure value, the maximum velocity value was about 37 m/s, while for the higher pressure value, it was about 45 m/s. In all cases considered, the highest velocity occurred in the core of the flow. Its value decreased gradually as it approached the walls due to fluid viscosity. In the case of the simple orifice geometries (A and B), little turbulence combined with the deceleration of the liquid near the orifice wall was observed. This phenomenon began just behind the orifice inlet which is also the starting point of the essential phase of hydrodynamic cavitation. The lowest velocity results from the formation of the gas phase with the chaotic movement of molecules that, in turn, significantly reduces velocity due to the resulting turbulent flow.

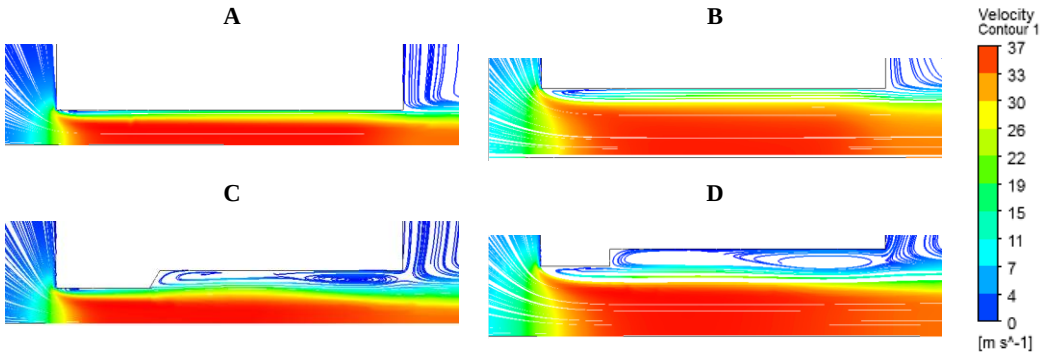

Fig. 3. Distribution of the fluid velocity for the tested orifices for the inlet pressure of 700 kPa

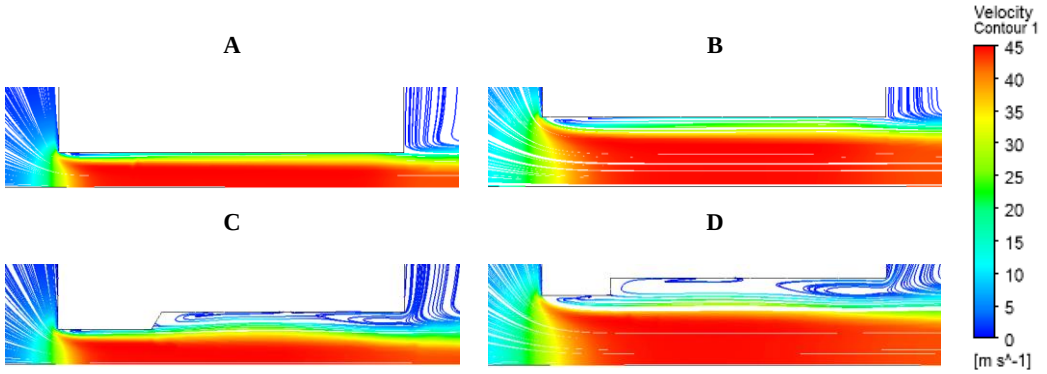

Fig. 4. Distribution of the fluid velocity for the tested orifices for the inlet pressure of 1 000 kPa

The other of the analyzed parameters was pressure distribution. The results for the studied orifices and pressures are shown in Fig. 5 and Fig. 6. According to Bernoulli's law and the continuity equation for fluid flow, the pressure value decreased due to the narrowing of the channel the fluid flows through. The local pressure drop was so significant that the static pressure value fell below the defined saturated vapor pressure, i.e. 3 570 Pa, and the phenomenon of hydrodynamic cavitation occured. For all geometries considered, the lowest pressure value (below the saturated vapor pressure) was obtained just behind the inlet edge in the near-wall layer zone. For geometry C, the area of the lowest pressure also occurred in the near-wall layer near the orifice diameter change. For the higher inlet pressure (1 000 kPa), the area of the lowest pressure was slightly larger than that of the lower inlet pressure (700 kPa). The pressure distribution in the flow core near the orifice inlet was approximately parabolic.

The last distribution analyzed was the volume fraction of the gas phase. The values of this parameter for the inlet pressures of 700 and 1 000 kPa and the tested geometries are shown in Fig. 7 and Fig. 8. In the case of the straight channels (orifice A and B), the zone of occurrence of the gas phase started just behind the inlet edge of the orifice and had the form of a near-wall layer. The diameter of the orifice increased due to the slight increase in the thickness of this layer. The varying cross-section of the orifice significantly increased the size of the zone where the gas phase occurs. The increasing diameter slightly increased its size. A similar effect was caused by the increased inlet pressure value.

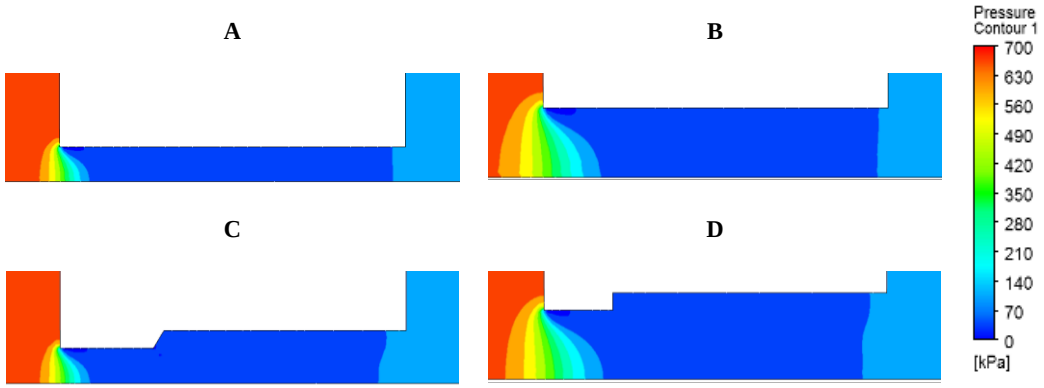

Fig. 5. Distribution of the fluid pressure for the tested orifices for the inlet pressure of 700 kPa

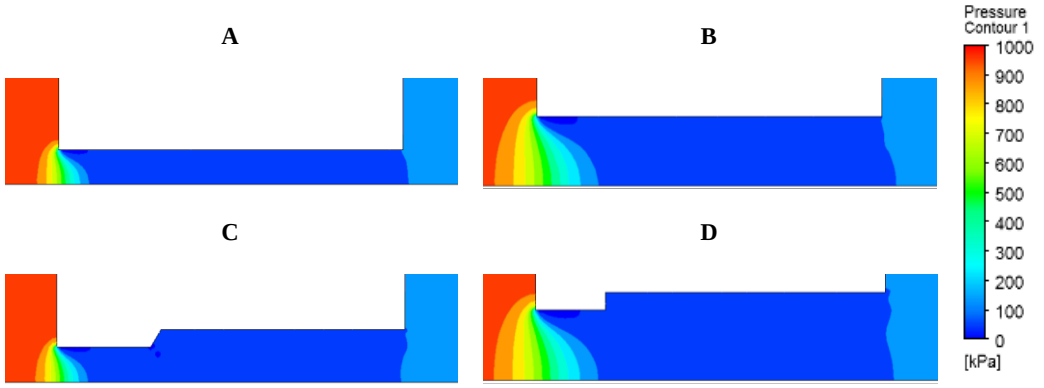

Fig. 6. Distribution of the fluid pressure for the tested orifices for the inlet pressure of 1 000 kPa

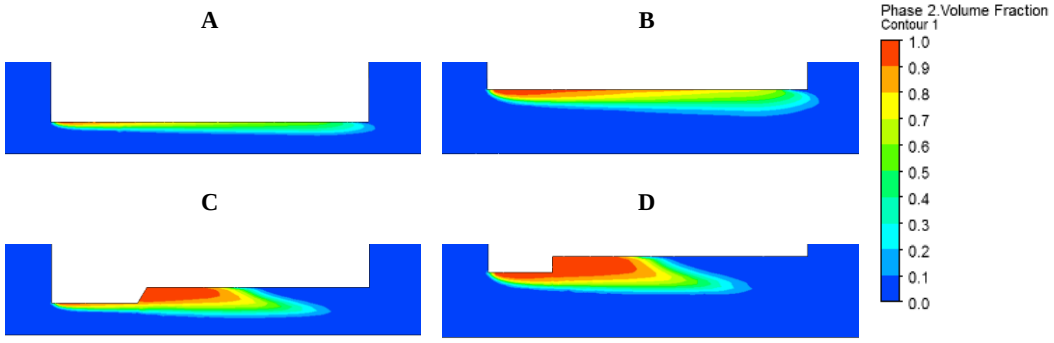

Fig. 7. Distribution of the volume fraction of the gas phase for the tested orifices for the inlet pressure of 700 kPa

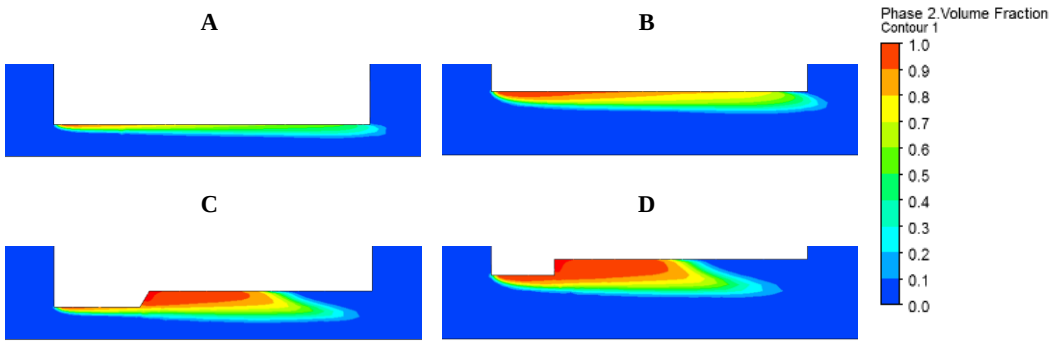

Fig. 8. Distribution of the volume fraction of the gas phase for the tested orifices for the inlet pressure of 1 000 kPa

The total volume fraction of the gas phase was further analyzed for the defined orifice geometries and inlet pressures (Fig. 9). The highest volume fraction was obtained for orifice D with a sharp change in its cross-sectional diameter, while the lowest volume fraction for geometry A with a straight channel of 1 mm diameter. It was also observed that the pressure value slightly affected the analyzed parameter. The most significant difference, i.e. more than 20% was observed for geometry D, while the smallest effect, i.e. 3% difference occurred for geometry A. The results obtained for geometry A may be due to the dominating influence of viscous forces in the fluid, which makes it difficult to change the state. In the case of geometry D, the larger diameter and its sharp increase provide more favorable conditions for cavitation initiation and its further development.

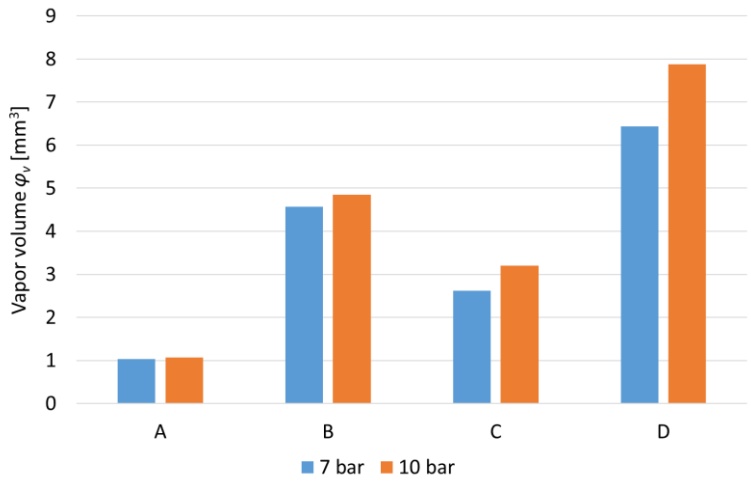

Fig. 9. Vapor volume for the selected orifices and defined inlet pressure values

Eventually, the vapor volume per power unit was calculated for the selected orifices and defined inlet pressure values (Fig. 10). Effective flow power was determined as the product of the vapor volume flow rate and the pressure difference at the inlet and outlet. Although geometry D provides the highest absolute value of vapor volume, considering the energy

flow associated with the fluid flow, the highest value of gas phase volume per unit power (0.24 mm^3/W) was obtained for geometry C and the lower pressure value. For the higher pressure, the parameter considered was 32% lower. The least favorable was geometry A, for which the volume fraction of the gas phase per unit power was 63% lower compared to geometry C (0.09 mm^3/W for 700 kPa).

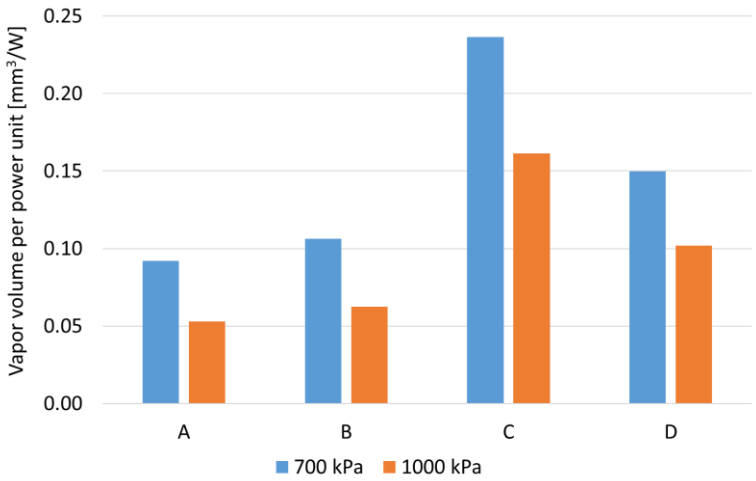

Fig. 10. Vapor volume per power unit for the selected orifices and defined inlet pressure values

4. CONCLUSION

This paper presents the results of a numerical study of the hydrodynamic cavitation phenomenon occurring as water flows through an orifice. Four orifice geometries were studied for two inlet pressure values, and the velocity, pressure, and volume fraction distributions obtained from the CFD simulations were analyzed.

The research made it possible to determine the location and size of the cavitation zone in the orifice cross-section. It was noted that cavitation initiation occurs just behind the inlet edge near the wall. The gas phase then develops as a stream located in the wall layer. This may result from the simultaneous influence of viscosity and turbulence associated with the rapid phase change of the fluid from liquid to gas.

For all geometries considered, the chaotic movement of particles in the wall layer zone generated by the phase transition resulted in a significant reduction in velocity to a value close to zero. For a higher inlet pressure value (1 000 kPa), a higher maximum flow velocity through the orifice was obtained (an increase of 8 m/s). This value occurred in the flow core at the axis of symmetry.

The lowest pressure value below the saturated vapor pressure occurred just behind the inlet edge in the near-wall layer zone for all the orifice geometries considered. This shows that the cavitation phenomenon (phase transition) started at the same spot regardless of the geometry. In the case of geometry C, the additional area with the lowest pressure occurred in the near-wall layer zone where the diameter changes, which means that the pressure drops due to flow acceleration resulting from the local change in geometry were large enough to exceed the saturated vapor pressure.

Using geometries with variable orifice diameters (C and D) resulted in a larger gas phase area. The most significant volume fraction of the gas phase in the considered computational domain was obtained for geometry D – a larger diameter orifice with its sharp increase. The smallest fraction was obtained for the straight orifice with a diameter of 1 mm (geometry A). The value of inlet pressure did not significantly affect the velocity near the cavitation zone. For the analyzed orifice geometries, a slightly higher volume fraction of the gas phase was obtained for the higher inlet pressure, with the largest difference (more than 20%) observed for geometry D. The largest value of the volume fraction of the gas phase per unit power was obtained for geometry C and the lower pressure value. This parameter was equal to 0.24 mm^3/W. The least favorable was geometry A for which this parameter was by 63% smaller than for geometry C.

The study allowed for a quantitative and qualitative evaluation of hydrodynamic cavitation in the tested orifice geometries. The orifice geometry with a diameter of 2 mm with a sharp increase in diameter (type D) generates the largest cavitation zone, and thus the largest volume fraction of the gas phase. This fact may result in a proportional increase in free radicals which will further react with substances in contaminated water. The results obtained enable further experimental studies to evaluate the efficiency of the wastewater treatment process.

Funding

The publication was financed by the Polish National Centre for Research and Development (grant agreement no. POIR.04.01.04-00-0057/20).

Acknowledgments

The work was performed within the framework of a project financed by the Polish National Centre for Research and Development (grant agreement no. POIR.04.01.04-00-0057/20).

Conflicts of Interest

The authors declare no conflict of interest.

REFERENCES

Brennen, C. E. (2011). *Hydrodynamics of pumps*. Cambridge University Press.

Capocelli, M., Musmarra, D., Prisciandaro, M., & Lancia, A. (2014). Chemical effect of hydrodynamic cavitation: simulation and experimental comparison. *AIChE Journal*, *60*(7), 2566–2572. https://doi.org/10.1002/aic.14472

Ding, H., Visser, F. C., Jiang, Y., & Furmanczyk, M. (2011). Demonstration and validation of a 3D CFD simulation tool predicting pump performance and cavitation for industrial applications. *Journal of fluids engineering*, *133*(1), 011101. https://doi.org/10.1115/1.4003196

Franc, J. P. (2006). *Physics and control of cavitation*. Grenoble Univ (France).

Gągol, M., Przyjazny, A., & Boczkaj, G. (2018). Wastewater treatment by means of advanced oxidation processes based on cavitation–a review. *Chemical Engineering Journal*, *338*, 599–627. https://doi.org/10.1016/j.cej.2018.01.049

Gogate, P. R., & Pandit, A. B. (2000). Engineering design methods for cavitation reactors II: hydrodynamic cavitation. *AIChE Journal*, *46*(8), 1641–1649. https://doi.org/10.1002/aic.690460815

Gogate, P. R., Tayal, R. K., & Pandit, A. B. (2006). Cavitation: a technology on the horizon. *Current science*, *91*(1), 35–46.

Gogate, P. R., Thanekar, P. D., & Oke, A. P. (2020). Strategies to improve biological oxidation of real wastewater using cavitation based pre-treatment approaches. *Ultrasonics Sonochemistry*, *64*, 105016. https://doi.org/10.1016/j.ultsonch.2020.105016

Iannetti, A., Stickland, M. T., & Dempster, W. M. (2016). A CFD and experimental study on cavitation in positive displacement pumps: Benefits and drawbacks of the 'full'cavitation model. *Engineering Applications of Computational Fluid Mechanics*, *10*(1), 57–71. https://doi.org/10.1080/19942060.2015.1110535

Kunz, R. F., Boger, D. A., Chyczewski, T. S., Stinebring, D., Gibeling, H., & Govindan, T. (1999). Multi-phase CFD analysis of natural and ventilated cavitation about submerged bodies. In *Proceedings of the 3rd ASME-JSME Joint Fluids Engineering Conference*. American Society of Mechanical Engineers.

Menter, F. (1993). Zonal two equation kw turbulence models for aerodynamic flows. In *23rd fluid dynamics, plasmadynamics, and lasers conference* (p. 2906).

Menter, F. R. (1994). Two-equation eddy-viscosity turbulence models for engineering applications. *AIAA journal*, *32*(8), 1598–1605.

Moholkar, V. S., & Pandit, A. B. (1997). Bubble behavior in hydrodynamic cavitation: effect of turbulence. *AIChE Journal*, *43*(6), 1641–1648.

Omelyanyuk, M., Ukolov, A., Pakhlyan, I., Bukharin, N., & El Hassan, M. (2022). Experimental and Numerical Study of Cavitation Number Limitations for Hydrodynamic Cavitation Inception Prediction. *Fluids*, *7*(6), 198. https://doi.org/10.3390/fluids7060198

Patil, P. B., Bhandari, V. M., & Ranade, V. V. (2021). Improving efficiency for removal of ammoniacal nitrogen from wastewaters using hydrodynamic cavitation. *Ultrasonics Sonochemistry*, *70*, 105306. https://doi.org/10.1016/j.ultsonch.2020.105306

Salvatore, F., Streckwall, H., & Van Terwisga, T. (2009). Propeller cavitation modelling by CFD-results from the VIRTUE 2008 Rome workshop. In *Proceedings of the first international symposium on marine propulsors, Trondheim, Norway* (pp. 22–24).

Sauer, J., & Schnerr, G. H. (2001). Development of a new cavitation model based on bubble dynamics. *ZAMM-Journal of Applied Mathematics and Mechanics/Zeitschrift für Angewandte Mathematik und Mechanik*, 81(S3 S3), 561–562. https://doi.org/10.1002/zamm.20010811559

Schnerr, G. H., & Sauer, J. (2001). Physical and numerical modeling of unsteady cavitation dynamics. In *Fourth international conference on multi-phase flow* (Vol. 1). ICMF New Orleans.

Shi, H., Li, M., Nikrityuk, P., & Liu, Q. (2019). Experimental and numerical study of cavitation flows in venturi tubes: From CFD to an empirical model. *Chemical Engineering Science*, *207*, 672–687.

Singhal, A. K., Athavale, M. M., Li, H., & Jiang, Y. (2002). Mathematical basis and validation of the full cavitation model. *J. Fluids Eng.*, *124*(3), 617–624. https://doi.org/10.1115/1.1486223

Subhas, S., Saji, V. F., Ramakrishna, S., & Das, H. N. (2012). CFD analysis of a propeller flow and cavitation. *International Journal of Computer Applications*, *55*(16), 26–33.

Tao, Y., Cai, J., Huai, X., Liu, B., & Guo, Z. (2016). Application of hydrodynamic cavitation to wastewater treatment. *Chemical engineering & technology*, *39*(8), 1363–1376. https://doi.org/10.1002/ceat.201500362

Wang, B., Su, H., & Zhang, B. (2021). Hydrodynamic cavitation as a promising route for wastewater treatment–A review. *Chemical Engineering Journal*, *412*, 128685. https://doi.org/10.1016/j.cej.2021.128685

Zheng, X. B., Liu, L. L., Guo, P. C., Hong, F., & Luo, X. Q. (2018, July). Improved Schnerr-Sauer cavitation model for unsteady cavitating flow on NACA66. *IOP Conference Series: Earth and Environmental Science*, *163*(1), 012020).

Zwart, P. J., Gerber, A. G., & Belamri, T. (2004, May). A two-phase flow model for predicting cavitation dynamics. In *Fifth international conference on multi-phase flow, Yokohama, Japan* (No. 152).